JMEPEG (2003) 12:715-720

Carbon Segregation and Inclusions Effects on Surface Fracture Morphology of a 12% Chromium Stainless Steel

N. Souami, D. Saidi, M. Negache, and A. Ati

(Submitted 18 March 2003; in revised form 27 June 2003)

Martensitic 12% chromium stainless steel is generally used for the manufacture of water vapour turbine blades. This material, under these environmental conditions, develops fatigue corrosion with failure as a result of the segregation of certain constituent elements such as phosphorus (P) and sulphur (S),[1-3] or the presence of some types of inclusions.[2-4] To be able to understand and explain these phenomena, in situ characterization of the fractured surfaces were performed for two types of samples: steel 1 as manufactured turbine material whose fracture mode is intergranular and steel 2 issued from last stage turbine blades after 100 000 h service at 40 °C whose fracture mode is transgranular. The techniques used for characterization were scanning electron microscopy (SEM) coupled with the x-ray analysis by energy dispersive spectroscopy (EDS), and auger electron spectroscopy (AES). The Auger results enabled the understanding of the brittle to ductile transition for the material by showing the simultaneous diffusion of carbon from grain boundaries (GB) to grains (G) and chromium from G to GB. Furthermore, the heavy segregation of phosphorus at the GBs could explain the intergranular crack rupture traces observed in steel 2. SEM observations coupled with EDS analysis showed the presence of different types of non-metallic inclusions such as silicon-based complex inclusions and manganese sulfides (MnS). The presence of silicon-based complex inclusions at GB could explain the intergranular fracture mode previously reported. The characterization of the fracture appearance suggests also that MnS inclusions can act as nucleation sites for secondary microcracks at the GB level that were observed after service.

Keywords inclusions, segregation, stainless steel, surface fracture

1. Introduction

Steam turbine blades are made of martensitic stainless steel with 12% chromium content. Since they contain high strength levels, this results in cracking and sometimes fatigue failures. Inclusions and impurities are present in this material, and in some cases, elements are deliberately added to improve mechanical properties. However, the presence of impurities such as phosphorus (P), carbon (C), sulphur (S), and non-metallic inclusions precipitation can be the source of fatigue crack initiation at grain boundaries.[1-5] During the use of 12% chromium stainless steel, an important phenomenon of the carbon segregation induces optimum fatigue conditions in the steels.[6-8] Mayes and Baker[9] suggest that the presence of the impurities like P, C, S, and the precipitation of MnS inclusions might initiate the fatigue crack at the grain boundary.

The current study investigates the effect of C, Cr, and P segregation and inclusions on the fracture mode of the material.

N. Souami, Centre Recherche Nucléaire d'Alger, Département de Caractérisation DTN CRNA, B.P. 1016 Alger, Algeria; **D. Saidi** and **M. Negache,** Centre Recherche Nucléaire de Draria, Département de Métallurgie, DMCN CRND B.P. 43 Draria, Alger, Algeria; and **A. Ati,** Université de Bejaia, Algeria. Contact e-mail: saididj@yahoo.fr.

2. Experimental Procedure

The chemical composition of the material investigated in the current study is shown in Table 1. This study is based on the surfaces rupture characterization of two types of samples. One type comes from new turbine blade (steel 1) and the other one is taken from a system which has been operating for more than 100 000 h (steel 2). Both had undergone an austenization heat treatment at 1050 °C for 1 h then quenching with oil followed by another heat treatment at 625 °C for 1 h. All samples were subjected to Auger electron spectroscopy (AES) analyses using a PHI600 system (Perkin Elmer, Minnesota). For this purpose, specimens were prepared with a notch in the coarse grained zone for in-situ fracturing within the Auger instrument. Fracturing was done at liquid nitrogen temperature under a pressure of less than 10^{-9} torr with a notch for initiating the crack and determining the fracture modes on the exposed surfaces.

Microstructural characterization was performed on the frac-

Table 1 Typical Composition of the Steel as Manufactured, wt.%

C	N	Al	Si	Mn	P	S	Cr	Mo	Ni	Cu	Ti	V	Fe
0.21	0.01	0.02	0.45	0.74	0.05	0.003	12.4	1.1	0.77	0.12	0.35	0.03	bal.

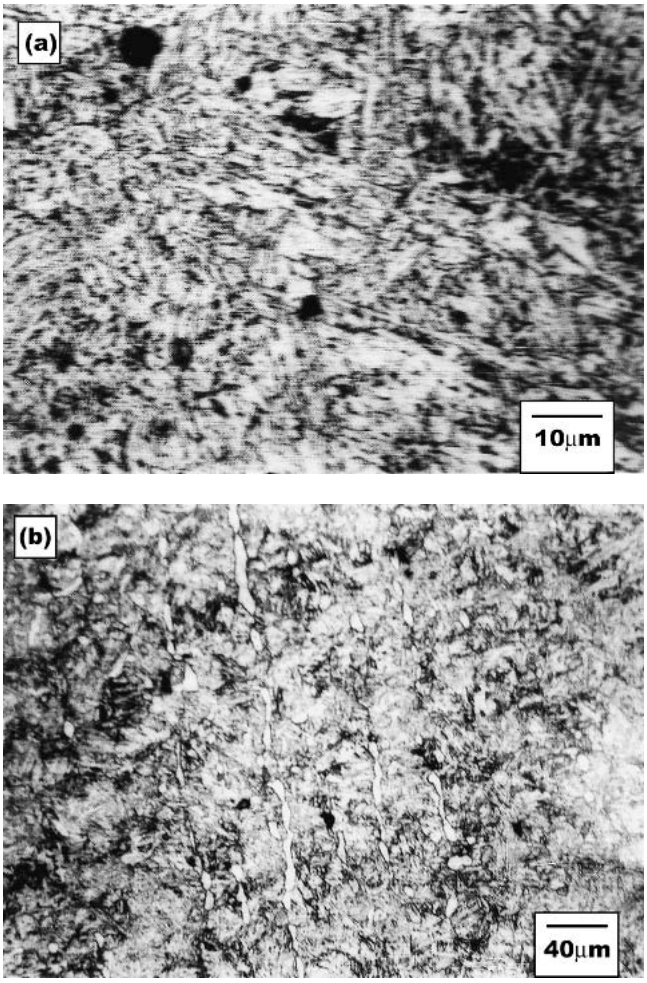

Fig. 1 Microstructure obtained after: **(a)** heat treatment at 625 °C; **(b)** 100 000 h service: apparition of aligned ferritic areas

tured surfaces using scanning electron microscope (SEM) associated to energy dispersive spectroscopy (EDS). The spectra were obtained by subtraction of the inclusion spectra from the matrix after normalization taking into account the FeK peak.

3. Results and Discussion

3.1 Microstructure

Figure 1(a) shows the material structure after heat treatment before use. It exhibits a martensite structure with the presence of chromium carbide particles of type $M_{23}C_6$ localized at the austenite grains boundaries and between the martensite lathes. After service (type 2), the ferritic areas dispersed in the martensitic structure become apparent. Theses areas, generally aligned in the stress direction during service (Fig. 1b), arise from the evolution of the martensite structure, under the effect of cyclic mechanical stress. The material undergoes hardening by transformation, which generates new hardened ferritic phases. These develop generally from non-metallic inclusions and on carbides too.[10]

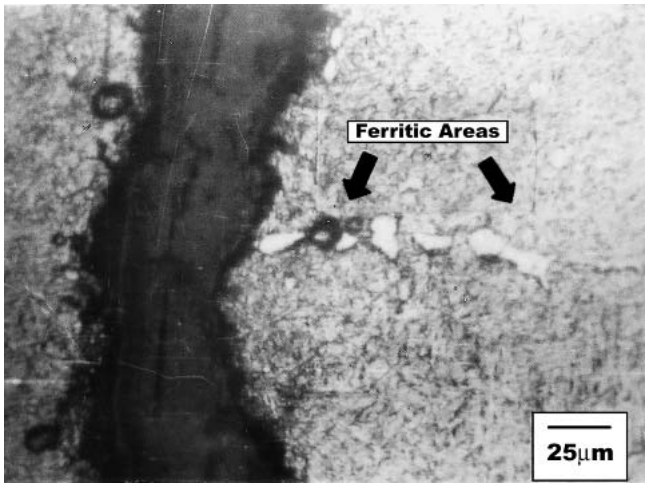

Fig. 2 Cross sectional view of splitting occurring perpendicularly to the aligned of ferritic areas

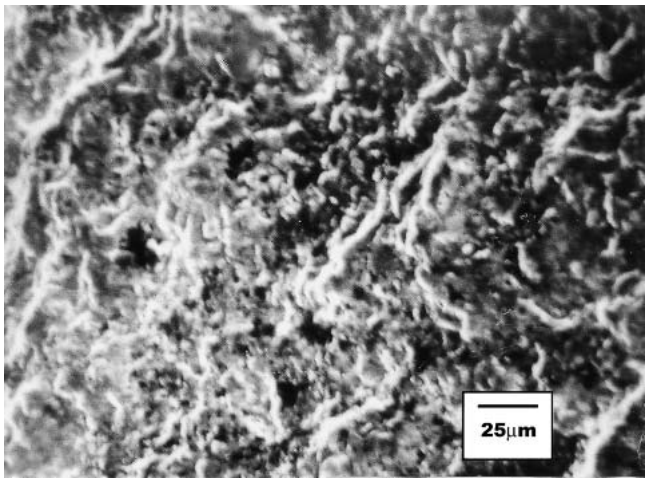

Fig. 3 Scanning electron fractograph showing fracture surface of splitting

3.2 SEM Investigations

3.2.1 Crack Examination. After a 100 000 h service, some blades develop cracking. Metallographic observation of the cracking regions shows that their direction is normal to the direction of ferritic areas (Fig. 2). Furthermore, it is known that ferritic areas embedded in martensite represent the most ductile phase, which accommodates in a first step the plastic deformation. The work of Degallaix et al.[10] on a martensitic stainless steel 12 Cr-Mo-V shows that the plastic deformation starts at the first cycle in the ferrite before it reaches martensite. Consequently, ferrite might be the start of the initiation of crack. On the other hand, Knutsen and Hutchings[11] observed that fatigue cracks in 12% chromium stainless steel propagate at ferrite grains boundaries.

We observed that cracks do not propagate along and between the ferritic areas; this suggests that their initiation and propagation is related to some other phenomena. On the other

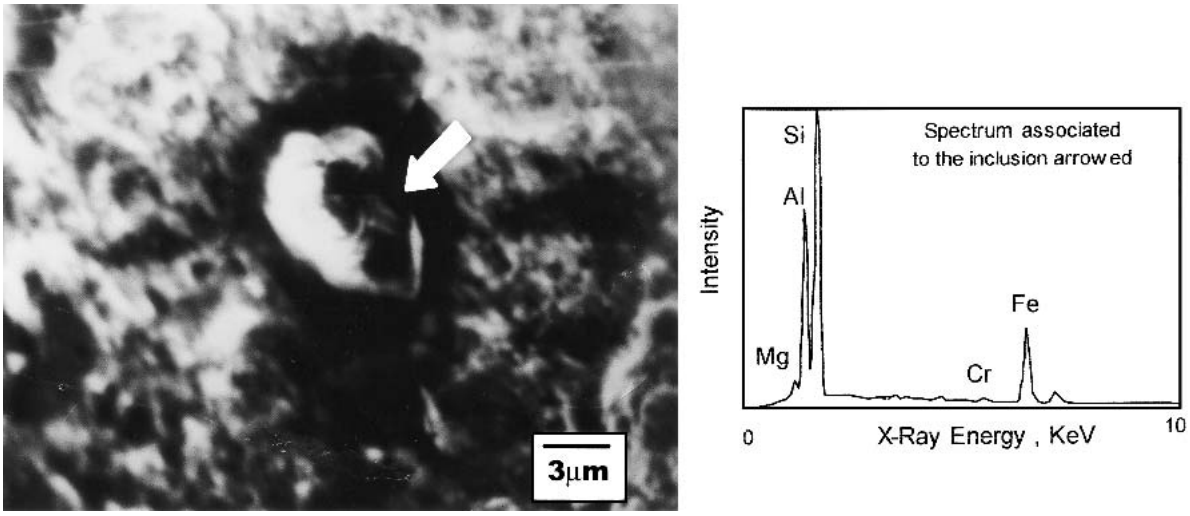

Fig. 4 Scanning electron fractograph showing a silicon-based complex inclusion

hand, cracks propagate along rich silicon area. The examination of crack areas shows a transgranular mode associated to some intergranular mode (Fig. 3).

The micrograph on Fig. 4 shows the presence of angular inclusions on fracture surface, which are identified by EDS as silicon-based complex inclusions combined with aluminium and iron. This seems to be the origin of crack initiation, and certainly facilitates the crack propagation. The angular form of these inclusions facilitates more the decohesion of the matrix-inclusion interface which can be the source of crack initiation. The stress field is certainly highly modified around these hard inclusions, which facilitates crack initiation when it is located in a region of high stress. An inclusion harder than the matrix with a high young modulus lowers the macroscopic stress for initiation, even though situated at several microns below the surface.[4]

3.2.2 In-Situ Fracture. After in-situ fracture, the heat-treated steel presents a brittle fracture of the intergranular type with ductile areas. The intergranular mode is characterized by a smooth grain surface (Fig. 5). Inclusions such as manganese oxide and aluminium- and silicon-based complex inclusions were observed on the fractured surface. Figure 6 shows the microcrack initiation at the interface of a spherical silicon-based inclusion and the matrix at the grain boundary. This observation shows the negative effect of this type of inclusion on crack initiation and on the intergranular mode of fracture. Besides other cited types of inclusions, these contribute to the crack propagation along the grain boundaries.

On the other hand, samples of type 2 show dimpled structure characteristic of a ductile fracture with a predominantly transgranular mode with some intergranular mode (Fig. 7a). The magnification of grain boundary (Fig. 7b) shows the presence of small cavities, which can be the mark of a previous localization of $M_{23}C_6$ carbides. The intergranular mode observed can be linked to the decohesion of the carbide from the matrix.

The crack surface area examination revealed only MnS type inclusions at grain boundary with microcrack initiation all around (Fig. 8). These suggest that MnS inclusions might originate from secondary crack initiation. Moreover, they contradict the conclusions of some authors who consider that these inclusions only facilitate propagation in the case of notched samples in which there is a reduced bulk and no oxide.[4] On the other hand, this result is in agreement with the result of Mayes and Baker[9] who concluded that MnS inclusions are responsible for fatigue microcrack initiation, which develops inside the crack stress field at the head of the major crack. Also, Horn et al.[2] showed that microcracks are always initiated at MnS inclusions and the propagation of intergranular cracks are accelerated by weakening elements such as phosphorus near these inclusions, and particularly at the matrix-inclusions interface. This explains to some extent the microcrack initiation at the MnS/matrix interface, which we observed.

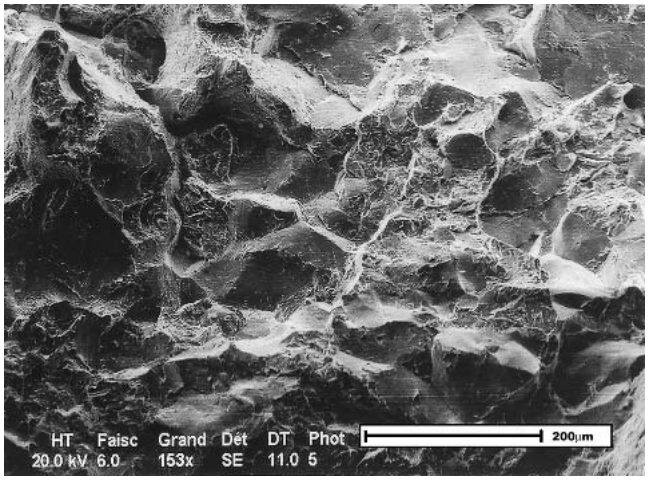

Fig. 5 Fracture surface micrography of the heat-treated material (steel)

3.3 AES and Fracture Surface Investigations

3.3.1 Steel 1. The crack path of the fractured samples observed under Auger examination was mainly intergranular. The

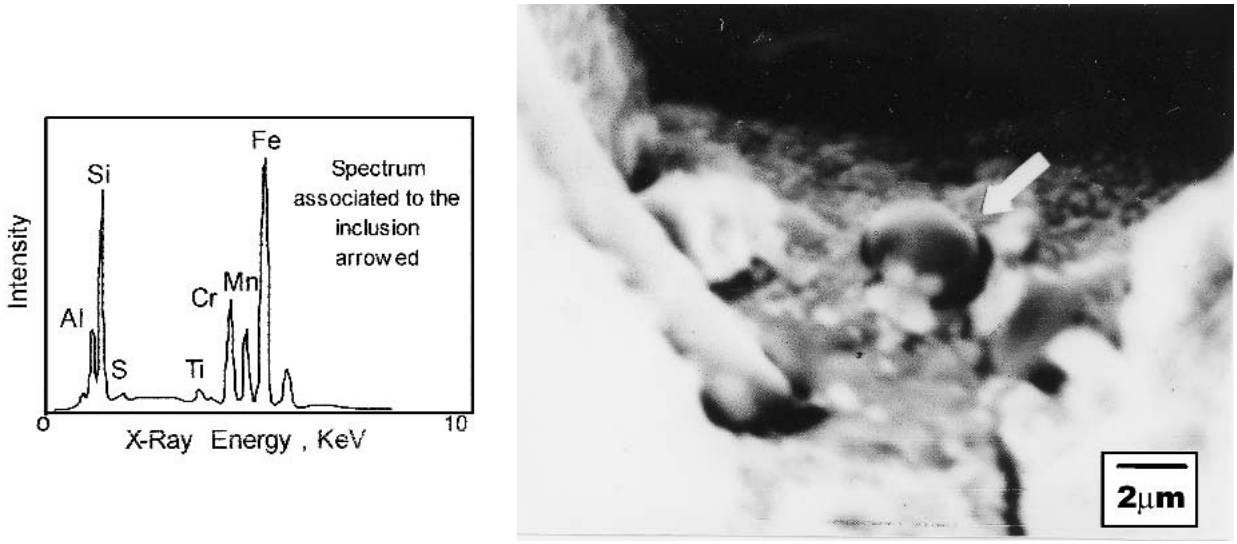

Fig. 6 Scanning micrograph showing microcrack initiation at a silicon-based complex inclusion

appearance of the fracture surface was predominantly smooth (Fig. 5). A noticeable carbon and chromium enrichment in the grains boundaries was detected. The typical line-Auger spectrum of such a surface, as shown in Fig. 9 and Fig. 10, represents the evolution of the Auger signals for C and Cr as a function of distance on one of the fractured surface. In addition, AES survey scans from 0-1000 eV were conducted to detect the presence of impurities with Auger peaks in this energy region. Only traces of sulphur were detected by Auger peak localized at 152 eV with sulphur ones at the same proportion in all areas of the exposed surface. Furthermore, the spectra showed only low intensity Auger signals for carbon (C) and chromium (Cr) at 270 and 490 eV inside the grain structure for steel 1 (Fig. 11). Significant changes in the intensity of the Auger peaks for C and Cr were observed in the grain boundary zone (Fig. 12). The AES intensity peak height related to the dN (E)/dE spectra was measured on steel 1 and steel 2 and used to estimate the concentration ratio of C and Cr between the grain center and the grain boundary regions. The computed results indicate that the grain boundary in steel 1 is considerably richer in carbon and chromium than in the grain, with a proportionality factor equal to 0.84 and 0.61, respectively, for C and Cr (Table 2). The partly high oxygen enrichment at the intergranular area of the fracture specimen is probably because some grain boundaries were sufficiently separated to provide a connection path to the atmosphere.

3.3.2 Steel 2. The same Auger analysis was carried out for steel 2 .The appearance of the fracture surface of steel 2 was different from that of steel 1; whereas steel 1 was predominantly smooth, steel 2 was characterized by a dimpled structure. The fractographic observation of Fig. 7(a) reveals a number of facets and cavities typically associated with a transgranular structure with the presence of brittle areas. The Auger line profile (Fig. 10) and the punctual Auger analysis (Fig. 12) reveals a significant increase of chromium and a pronounced decrease in the concentration of carbon in the grain boundary region compared with that within the grain with an average ratio of 0.68 and 1.78.

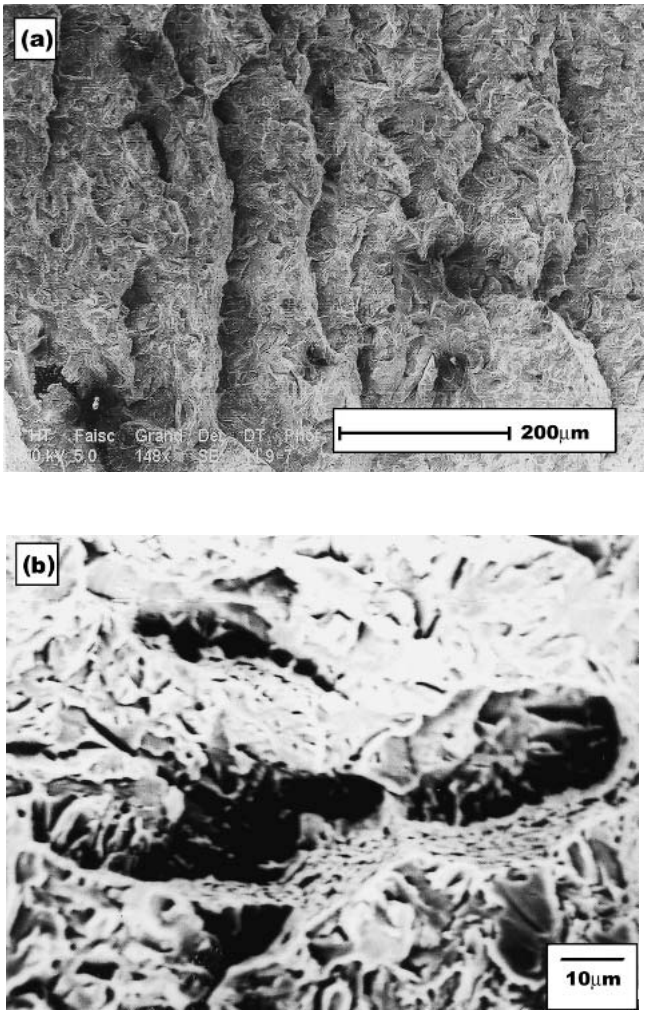

Fig. 7 Fracture surface of steel 2: **(a)** predominantly transgranular mode fracture, **(b)** presence of microvoids at grains boundaries

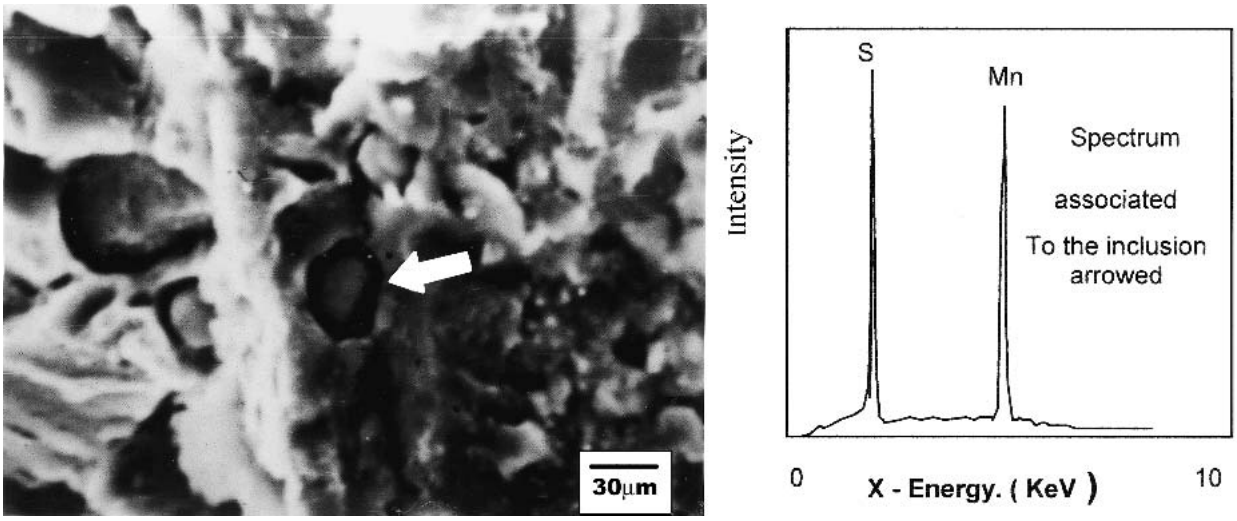

Fig. 8 Manganese sulphide inclusion exposed at grains boundary

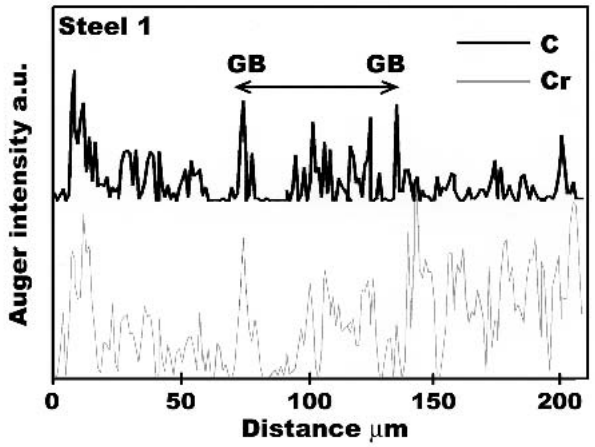

Fig. 9 AES line profile of carbon and chromium as a function of distance on the intergranular surface fracture (steel 1)

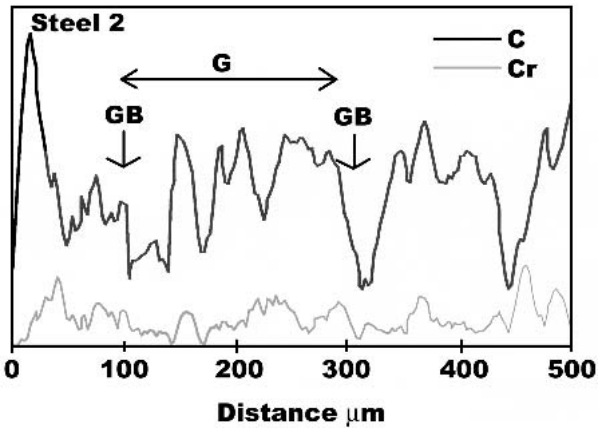

Fig. 10 AES line profile of carbon and chromium as a function of distance on the transgranular surface fracture (steel 2)

Therefore, the change in the structure could be attributed essentially to the segregation of carbon from the grain boundary region to the grain center during the operation of the material. Taking into account the atomic concentration ratio of C and Cr, respectively, in the grain center and the grain boundary region for steel 1 to that of steel 2 (Table 2), an enrichment factor equal to 2 is found for the carbon in the grain center whereas it is 1.15 for the chromium in the grain boundary region.

This investigation has also shown that carbon and chromium enrichment occurs at the grain boundary region, which leads to embrittlement fracture for original steel 1. For steel 2, at the early stage of the fatigue test, the segregation of carbon and chromium, respectively, at the grain center and the grain boundary regions, allows a ductile behavior of the material to take place with high resilience characteristics. The relative enrichment of the grain in carbon (multiplied by $\cong 2$) after fatigue induces a high segregation of phosphorus at G and GB as shown by the AES punctual analysis (Fig. 11, 12). The inclusions associated with these fracture modes were too small in most cases to be detected by integral Auger analysis.

4. Conclusion

The study of crack surface with SEM investigations of treated heat turbines blades type 1 or 2 lead to the following conclusions:

- Ferrite is not the origin of initiation and propagation of cracks. The matter is mainly due to the presence of silicon-based complex inclusions, which also facilitate propagation.
- The intergranular fracture observed after heat treatment is the result of the presence of various inclusions such as silicon-based complex ones. These represent secondary crack initiation sites localized at grain boundaries.
- The intergranular microcrack observed after fatigue is due to the presence of MnS type inclusions.

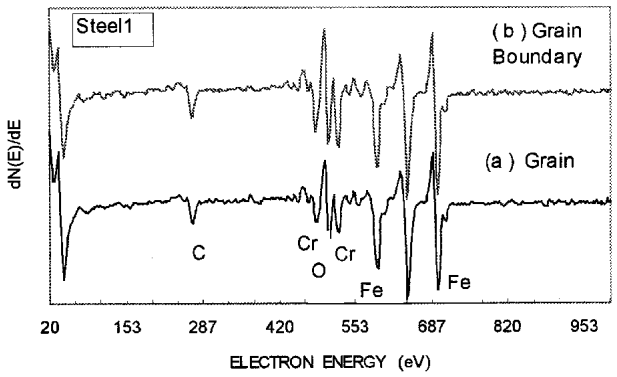

Fig. 11 AES spectra of steel 1 representing: **(a)** the grain, and **(b)** the grain boundary obtained from the intergranular fracture

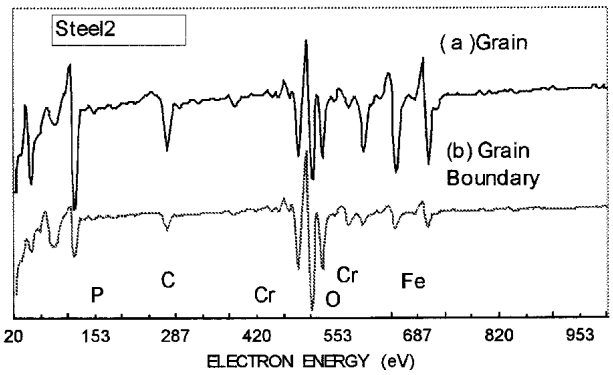

Fig. 12 AES spectra of steel 2 representing: **(a)** the grain, and **(b)** the grain boundary obtained from the transgranular fracture

Table 2 Atomic % Ratio (X) of Carbon (C) and Chromium (Cr) in the Grain Center (G) to the Grain Boundary Region (GB) for Steel 1 and 2, Calculated by Seah et al.[12] Formula and Sensitivity Factors

Steel	1	2
X_C (G)/X_c (GB)	0.84	1.78
X_{cr} (G)/X_{cr} (GB)	0.61	0.68

The results that were obtained for Auger fractured samples were as follows:

1) Fracture mode:

- for steel 1: the fracture was brittle with an intergranular mode and the presence of ductile areas.
- for steel 2: the fracture was ductile with a transgranular mode and presence of traces of an intergranular mode fracture.

2) Auger analysis:

- The Auger results allowed us to understand the brittle to ductile transition for the material by showing the simultaneous diffusion of carbon from grain boundary region (GB) to grain center (G) and chromium from (G) to (GB). Furthermore, the heavy segregation of phosphorus at the grain boundaries explained the intergranular crack rupture traces observed in steel 2.

References

1. A. Pineau and J.L. Castagné: "Influence of Intercrystalline Fracture Associated With Temper Brittleness on the Rate of Fatigue Crack-Propagation in Martensitic Steel With 12-Percent-Cr," *Mém. Et. Sci. Rev. Metall.*, 1979, *6,* pp. 369-76.
2. H. Horn, T. Pintat, V. Schlett, and H. Weiss: "Influence of Phosphorus and Sulphur Segregation on Stress Relief Cracking," *Scanning Microsc.,* 1988, *2,* pp. 767-75.
3. T.A. Khalifa: "Effect of Inclusions on Fatigue Limit of a Heat-Treated Carbon-Steel," *Mater. Sci. Eng. A,* 1988, *102,* pp. 175-80.
4. C. Gasc, B. Bouchet, and R. Moussaddyki: "Etude Fractographique de la Rupture de l'Acier 30CD4. Effets des Inclusions sur les Mécanismes de la Rupture," *Mem. Et. Sci. Rev. Met.,* 1988, *197,* pp. 387-96.
5. J.J. Lewandowski, C.A. Hippsley, and J.F. Knott: "Effects of Impurity Segregation and Test Environment on Sustained Load Cracking of 2 1/4 Cr-1Mo Steel-Crack Propagation," *Acta Metall.,* 1987, *35,* pp. 2081-90.
6. I.M. Yongbin and S. Danyluk: "A Surface Segregation Study in Phosphorus and Sulfur-Doped Type 304 Stainless Steels," *Metall. Trans. A.,* 1987, *18A,* pp. 19-26.
7. S. Danyluk and J.Y. Park: "Low Temperature Intergranular Fracture and Grain-Boundary Chemistry of Sensitized Type-304 Stainless Steel," *Scripta Metall.,* 1982, *16,* pp. 769-74.
8. S. Danyluk, J.Y. Hong, and I. Wolke: "Grain-Boundary Corrosion of Sulfur and Phosphorus Doped and Sensitized AISI-304 Stainless Steel," *Corrosion,* 1984, *40,* pp. 598-604.
9. I.C. Mayes and T.J. Baker: "Inclusion-Induced Anisotropy of Fatigue Crack Growth in Steel," *Mater. Sci. Technol.,* 1986, *2,* pp. 133-39.
10. G. Degallaix, J.B. Vogt, and J. Foct: "Fatigue Oligocyclique et Comportement Structural de l'Acier Inoxydable Martensitique 12CR-Mo-V," *Mem. Et. Sci. Rev. Métall.,* 1990, *87*, pp. 47-58.
11. R.D. Knutsen and R. Hutchings: "Occurrence of Non-Metallic Inclusion in 3CR12 Steel and Their Effect on Impact Toughness," *Mater. Sci. Technol.,* 1988, *4,* pp. 127-35.
12. M.P. Seah and W.A. Dench: "Quantitative Electron Spectroscopy of Surface. A Standard Data Base for Electron Inelastic Mean Free Paths in Solids," *Surf. Interf. Anal.,* 1979, *1,* pp. 2-11.